ChemComm

COMMUNICATION

View Article Online
View Journal | View Issue

Cite this: *Chem. Commun.*, 2025, **61**, 19485

Received 29th August 2025,
Accepted 11th November 2025

DOI: 10.1039/d5cc04995d

rsc.li/chemcomm

Mechanical deformations in battery current collectors observed by *operando* X-ray diffraction on Si/graphite anodes

Anders Brennhagen, *[a] Dipankar Saha, [a] Izar Capel Berdiell, [a] Andrew Pastusic Jr,[a] Marta Koposova,[b] David S. Wragg, [ab] Dennis Becker,[c] Dmitry Chernyshov, [d] Carl Erik Lie Foss [b] and Alexey Y. Koposov *[a]

Current collectors in Li-ion batteries are often considered passive components with minimal influence on performance. However, materials with large expansion during lithiation may influence the current collector. Herein, we demonstrate mechanical deformations of the Cu current collector in Si/graphite electrodes using *operando* X-ray diffraction.

The electrodes of Li-ion batteries (LIBs) are complex chemical systems comprising multiple components including active material(s), binder(s), conductive additive(s) and current collector. The vast majority of work in the field of battery materials primarily targets the chemistry of active materials.[1] Components considered inactive (conductive additives and current collectors) are rarely objects of study. The function of these components becomes increasingly important when active materials are subjected to large expansion/contraction during electrochemical cycling. Such changes are particularly pronounced for anode materials operating under alloying mechanism with silicon (Si) being the most studied example.[2]

Si has long been considered one of the most promising anode materials for LIBs due to its high capacity.[3] However, the fast capacity decay upon electrochemical cycling, linked to the large volumetric changes during (de)lithiation, impedes the widespread implementation of Si-based anodes in modern LIBs. Several strategies have been proposed to mitigate the degradation problems and improve the cycling stability of Si-based electrodes.[4] The most common strategy to stabilize the electrochemical performance of Si in LIBs is the fabrication of composite electrodes comprised of Si and graphite. Such electrodes have demonstrated an acceptable compromise between capacity and cycling stability.[5]

A more fundamental approach towards optimization of Si-based electrodes is gaining a complete understanding of the operating mechanism through various *operando* characterisation methods, which can be further used for targeted material optimization.[6–12] In the search for degradation mechanisms of the Si-based anodes most studies focus on the Si particles instead of the electrode as a whole. These works typically link the capacity degradation to cracking of Si particles during (de)lithiation due to large expansion/contraction, followed by growth of solid electrolyte interphase (SEI) and resistance build-up.[3]

An additional degradation process in Si-based anodes is the loss of active material due to detachment from the current collector.[13] It is commonly accepted that this detachment is driven by mechanical stress originating from the lithiation of Si and the following expansion.[14,15] Studies have shown that modifications of the current collector surface, such as sanding, etching or electrochemical deposition of Cu onto the Cu current collector, can significantly reduce detachment of the active material.[16,17] In addition, thick current collector foils (18 μm *vs.* common 10 μm) have shown increased electrode stability and resistance towards detachment.[18] Mechanically induced lattice strain in Cu current collector in a commercial pouch cell with graphite anodes has previously been observed through *operando* XRD.[19] This study decoupled mechanical lattice strain from thermal expansion and estimated it to be ~0.0002 for this particular cell.[19] It has also been shown, through microscopic studies on Si thin film anodes, that lattice strain in Cu current collectors play an important role in the failure mode.[15,20] However, similar studies on conventional Si-based electrodes with binder(s) and conductive additive(s) are missing.

In this work, we offer new insights into the mechanical changes that occur in the Cu current collector during electrochemical cycling of Si/graphite composite electrodes. Through 19 *operando* XRD measurements, we demonstrate that the lattice strain of Cu during lithiation is coupled to the expansion of Si and may lead to

[a] *Centre for Materials Science and Nanotechnology, Department of Chemistry, University of Oslo, PO Box 1033, Blindern, 0315, Oslo, Norway. E-mail: anders.brennhagen@smn.uio.no, alexey.koposov@kjemi.uio.no*
[b] *Department of Battery Technology, Institute for Energy Technology (IFE), Instituttveien 18, 2007, Kjeller, Norway*
[c] *Bruker AXS SE, Oestliche Rheinbrueckenstr. 49, 76187 Karlsruhe, Germany*
[d] *Swiss-Norwegian Beamlines, European Synchrotron Facility, 71 Avenue des Martyrs, 38043 Grenoble, France*

loss of contact between the active materials and the current collector. This finding reveals an extra obstacle to achieving stable electrochemical performance during long term cycling of Si-based LIB electrodes.

We prepared the electrodes by a water-based procedure, described in Section S1 (SI) using crystalline Si, graphite, carboxymethyl cellulose (CMC), styrene-butadiene-rubber (SBR) and carbon black. To examine the roles of the Si/graphite ratio and total active mass loading (Si + graphite) on the behaviour of the current collector, we fabricated electrodes with varying Si amounts (20, 30, 40, 50 wt% Si) and active mass loadings (2–10 mg cm^{-2}). This compositional range was chosen to be able to observe significant differences in behaviour of the current collector without severely changing the electrode structure. *Operando* X-ray diffraction (XRD) measurements in transmission mode were conducted on 19 of these electrodes with Li metal as a counter electrode and 1.2 M $LiPF_6$ in 3 : 7 vol% ethylene carbonate : ethylmethyl carbonate (EC : EMC) with 10 wt% fluoroethylene carbonate (FEC) and 2 wt% vinylene carbonate (VC) as electrolyte. A selected example from these measurements is presented in Fig. 1 where an electrode with 30 wt% of Si was cycled at C/20 (based on the calculated theoretical capacity of the electrode). Here, the peaks corresponding to Cu ((111) and (200) reflections) are highlighted, while all other Bragg reflections from the cell are omitted for clarity. The *operando* XRD during the first lithiation revealed a shift of the Cu reflections first towards lower *Q* values, indicating an increase in lattice parameter, and then back towards higher *Q* values. In this experiment, no clear changes to these peak positions were observed in the subsequent cycles.

To verify that the observed shifts in Cu reflections stemmed from changes in lattice parameters, rather than sample displacement, we conducted two *operando* XRD measurements under identical conditions with different orientations of the battery stack. In one experiment, the cell was assembled with the Si/graphite electrode facing the X-ray source, while in the other, the electrode faced the detector (Fig. S3, SI). In the case of peak shifts originating from sample displacement, the diffraction peaks would shift in opposite directions for the two different orientations. Instead, both configurations revealed peak shifts in the same direction, confirming that the observed changes in XRD patterns originated from actual changes in the Cu unit cell dimensions.

This change in the Cu unit cell dimensions could in principle have several origins, for example thermal expansion. However, this was deemed unlikely as the observed expansion would indicate a temperature increase of approximately 80 K.[21] For comparison, a recently reported cylindrical LIB cell has shown an internal temperature increase of ~40 K when cycled at a cycling rate of 10C, and only ~7 K at 2C.[22] This shows that the internal temperature of the cell has a high dependency on cycling rate, with faster cycling leading to higher temperature increase.[19,22] *Operando* XRD studies of lattice strain of Cu current collector in commercial cells with graphite anodes have also shown that thermal expansion is negligible compared to mechanical strain at low C-rates (<1C).[19,23] In accordance to this, we observed no clear difference in the *operando* XRD patterns between similar electrodes cycled at the much lower rates of C/10 and C/20 (Fig. 2).

To test if the movement of the Cu (111) and (200) reflections could originate from mechanical stretching, we performed a control experiment by applying various weight loads to a strip of Cu foil while measuring changes in the XRD pattern. This experiment confirmed that direct mechanical stretching of Cu exhibit similar changes in the XRD patterns as during cycling in the *operando* cells (Section S3, SI).

Through the 19 *operando* XRD measurements of electrodes with different loadings and Si/graphite ratios we observed similar Cu stretching to the example showed in Fig. 1. The extent of the changes was found to be strongly dependent on

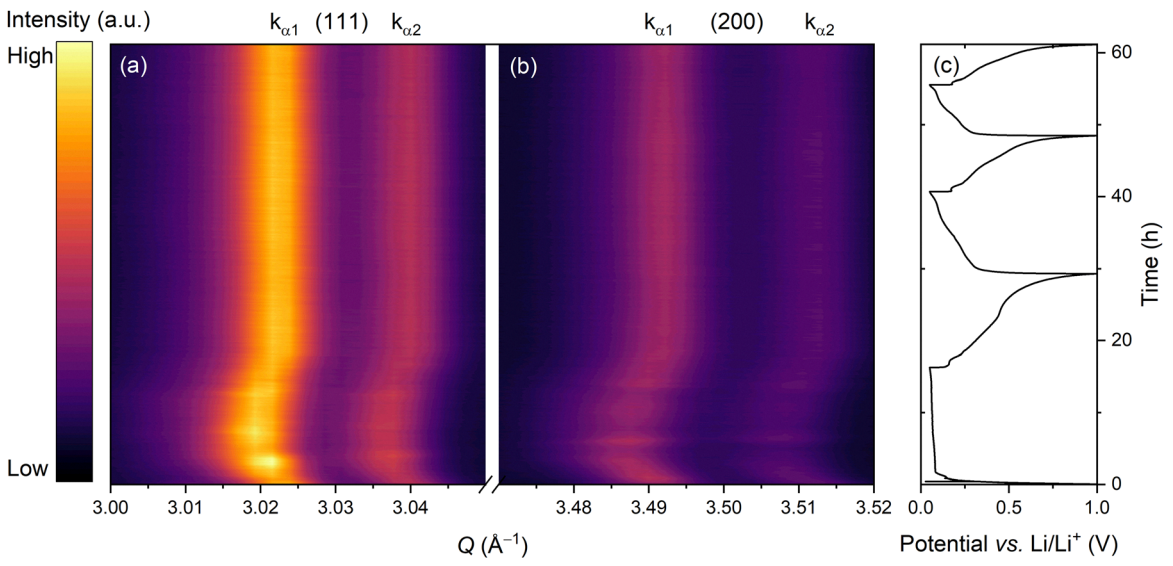

Fig. 1 (a) and (b) contour plots of the 111 and 200 diffraction peaks corresponding to the Cu current collector, respectively and (c) charge/discharge curves during *operando* measurement. The data was extracted from an *operando* XRD measurement of a Si/graphite based electrode cycled *vs.* Li metal with a cycling rate of C/20 and voltage range of 0.05–1.00 V *vs.* Li/Li^+. The figure shows the contributions from both Mo $k_{\alpha1}$ and $k_{\alpha2}$ radiation. The time axis showed in (c) is also valid for (a) and (b).

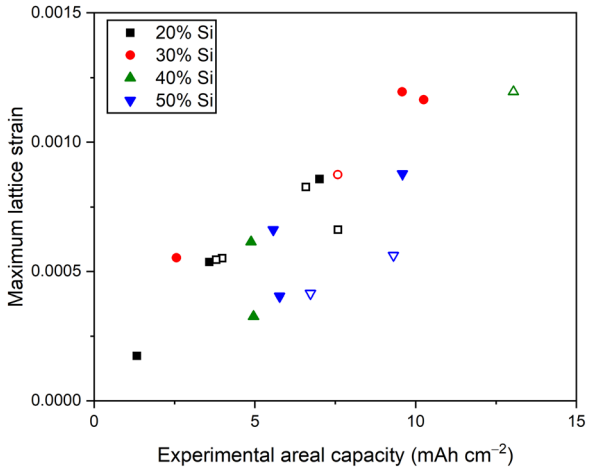

Fig. 2 Maximum lattice strain of the Cu current collector during the first lithiation as a function of experimentally measured areal capacity. The data is extracted from 19 *operando* XRD measurements of electrodes cycled in half cell configuration at either C/10 and 0.01–1 V *vs.* Li/Li$^+$ (open symbols) or C/20 and 0.05–1 V *vs.* Li/Li$^+$ (closed symbols). The correlation between theoretical and experimental capacity and the maximum lattice strain *vs.* active mass loading is shown in Fig. S5 (SI).

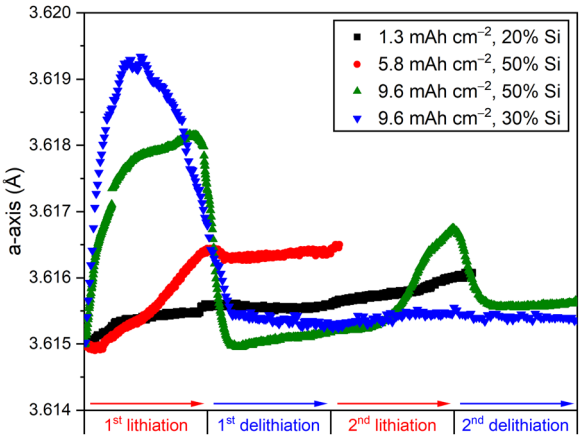

Fig. 3 Correlation between the unit cell parameter of Cu and lithiation/delithiation extracted from *operando* XRD measurements of four different cells cycled at C/20 and 0.05–1 V *vs.* Li/Li$^+$, showing different Cu expansion behaviours related to the experimental areal capacity of the 1st lithiation. The relative Si amount and experimental areal capacity are provided in the figure legend.

the electrode composition. The analysis of the *operando* XRD data provided an estimate of the maximum lattice strain (ε_a) of Cu during the first lithiation for each of the measurements through the following equation:

$$\varepsilon_a = \frac{a_{max} - a_0}{a_0}$$

Here a_{max} is highest *a*-axis value obtained during the first lithiation and a_o is the *a*-axis value extracted from the first XRD scan (Section S1, SI). This lattice strain proved to be generally larger for the electrodes with higher areal capacities, associated with higher active mass loading and a larger amount of Si (Fig. 2). The highest observed lattice strain was just below 0.0012, which is well within the elastic region for Cu (below ~0.003).[24] Therefore, no irreversible plastic deformation of the Cu foil should occur under these conditions.

To better correlate the changes in the unit cell of Cu with the electrochemical behaviour, we performed a detailed study of four electrodes with different areal capacities (Fig. 3 and Fig. S4, SI). The electrode with the lowest loading (1.3 mAh cm^{-2}, black symbols in Fig. 3) showed a slight increase in the Cu lattice parameter during the first lithiation and no significant changes after. During subsequent lithiation, only a small increase in the lattice parameter was observed. A higher areal capacity of 5.8 mAh cm^{-2} resulted in a higher increase in lattice parameter during the first lithiation (red symbols in Fig. 3), but no other clear differences compared to the electrode with 1.3 mAh cm^{-2}.

When increasing the areal capacity even more to 9.6 mAh cm^{-2} with 50% Si the maximum *a*-axis value was significantly larger (a_{max} = 3.61816(3) Å) and was followed by a rapid drop back to its original value (green symbols in Fig. 3). During the subsequent delithiation, the changes observed in the unit cell were negligible. This behaviour repeated itself during the second cycle, but with a significantly lower increase in lattice parameter (a_{max} = 3.61675(3) Å). In another example, with the same experimental areal capacity but with 30% Si, a slightly different behaviour was observed (blue symbols in Fig. 3). The increase in the Cu lattice parameter in this electrode was slightly larger (a_{max} = 3.61934(9) Å) and there was no significant change in *a*-axis value after the first lithiation. This observation indicates that stretching of Cu over a certain threshold (~3.619 Å) decreases the tendency of repeated stretching/relaxation in subsequent cycles. The difference between these two electrodes with 9.6 mAh cm^{-2} areal capacity could be explained by influence of thickness on the lithiation processes in the electrodes and the deformation of Cu.

These changes in lattice parameter can only be explained by stretching of Cu current collector along the plane due to expansion of the active materials within the electrode. Because of a positive Poisson's ratio of Cu this stretching along the plane should also lead to a contraction perpendicular to the plane. However, due to the geometry of the *operando* XRD measurements the sets of atomic planes that contract will likely not fulfil the Bragg condition and will therefore be invisible in our XRD measurements.

While the increase of the *a*-axis unit cell parameter of Cu corresponds to stretching of the current collector, the subsequent decrease (observed in Fig. 3) is most likely driven by a loss of the chemical connection between the active components and the current collector, allowing the current collector to relax back into its original state. The subsequent stretching and relaxation beyond the first cycle is an indication of the severity of this process: the contact loss is more severe for electrodes showing no changes in the unit cell parameters of Cu after the first lithiation (blue curve in Fig. 3) compared to electrodes showing repeated stretching and relaxation (green curve in Fig. 3). The maximum lattice strain observed in this dataset is 0.0012, which corresponds to an applied stress of ~160 MPa using a Youngs modulus of 130 GPa.[25]

Hence, this method could be used as an estimate for the adhesion strength between the current collector and the active components of the electrode. The loss of contact could lead to higher resistance, inactive areas of the electrode and could be a contributor to the poor cycling stability of Si-based anodes in addition to the already known problems of particle cracking and excessive SEI formation.[3] To avoid this loss of contact, surface modifications and morphology control of the current collector can be considered for future electrode optimization.[16–18]

We expect that deformation of current collectors will occur in most batteries during cycling. However, the magnitude and development of the lattice strain will depend on type and orientation of active material, electrode formulation, binder, solvent, mixing procedure, coating thickness, current collector thickness and morphology.[16,17] For example, lattice strain of Al and Cu current collectors has previously been observed in a commercial pouch cell with NMC cathode and graphite anode, but the measured values were significantly lower than what we observed in our Si/graphite electrodes.[19] This is explained by the larger volume expansion of Si compared to graphite and NMC and the higher capacity loadings used in this study, which are significantly higher than commercially relevant anodes.

In conclusion, we have demonstrated that the Cu current collector in Si/graphite electrodes undergoes mechanical deformation during electrochemical cycling. These observations were made based on 19 *operando* XRD measurements. The stretching is caused by the expansion of the active materials deforming the Cu foil and inducing a lattice strain observed as peak shifts in XRD. When the expansion of the active material becomes too large it can lead to loss of contact between the current collector and the active components allowing the Cu current collector to relax. We also demonstrated a correlation where the maximum lattice strain increases with areal capacity of the electrodes during the first lithiation. These findings highlight a potential limitation for electrodes based on active materials with large volume expansion during cycling.

This work has been primarily funded by the Research Council of Norway through the SUMBAT project (grant 328780) and through FME Battery (grant 350373). The authors acknowledge the use of the Norwegian national infrastructure for X-ray diffraction and scattering (RECX, grant 208896) and the Norwegian advanced battery laboratory infrastructure (NABLA, grant 322227). The Swiss-Norwegian Beamlines, ESRF, are acknowledged for providing beamtime and their staff with invaluable support. The authors thank Dr Vadim Diadkin (ESRF) for support and discussions and Dr Heesoo Park (UiO) for assistance with the graphics presented in this article.

Conflicts of interest

There are no conflicts to declare.

Data availability

The background data for this publication including input and result files for the refinements are openly available at dataverse.no.[26] The raw data files from the synchrotron measurements are archived at data.esrf.fr and will automatically be openly available in 2028 at latest.[27,28]

Supplementary information (SI): experimental details, additional XRD measurements. See DOI: **https://doi.org/10.1039/d5cc04995d**.

Notes and references

1 C. Hui, W. Yu-Rong, H. Xiao and Y. Ting-Feng, *Energy Mater.*, 2021, **1**, 100003.
2 S. V. Gopinadh, P. V. Phanendra, A. V, B. John and M. Td, *Energy Fuels*, 2024, **38**, 17253–17277.
3 H. Zhao, J. Li, Q. Zhao, X. Huang, S. Jia, J. Ma and Y. Ren, *Electrochem. Energy Rev.*, 2024, **7**, 11.
4 L. Sun, Y. Liu, R. Shao, J. Wu, R. Jiang and Z. Jin, *Energy Storage Mater.*, 2022, **46**, 482–502.
5 W. Zhang, P. Han, Y. Liu, X. Lin and Y. Wu, *FlatChem*, 2025, **50**, 100833.
6 K. Dong, H. Markötter, F. Sun, A. Hilger, N. Kardjilov, J. Banhart and I. Manke, *ChemSusChem*, 2019, **12**, 261–269.
7 S. N. S. Hapuarachchi, M. W. M. Jones, K. C. Wasalathilake, I. Marriam, J. Y. Nerkar, N. Kirby, D. P. Siriwardena, J. F. S. Fernando, D. V. Golberg, A. P. O'Mullane, J.-C. Zheng and C. Yan, *Small Methods*, 2024, **8**, 2301199.
8 P. Pietsch, M. Hess, W. Ludwig, J. Eller and V. Wood, *Sci. Rep.*, 2016, **6**, 27994.
9 P. Schweigart, W. Hua, P. A. Sánchez, C. Lian, I.-E. Nylund, D. Wragg, S. Y. Lai, F. Cova, A. M. Svensson and M. V. Blanco, *Small*, 2025, **21**, 2406615.
10 S. Tardif, E. Pavlenko, L. Quazuguel, M. Boniface, M. Maréchal, J.-S. lMicha, L. Gonon, V. Mareau, G. Gebel, P. Bayle-Guillemaud, F. Rieutord and S. Lyonnard, *ACS Nano*, 2017, **11**, 11306–11316.
11 D. S. Wragg, C. Skautvedt, A. Brennhagen, C. Geiß, S. Checchia and A. Y. Koposov, *J. Phys. Chem. C*, 2023, **127**, 23149–23155.
12 P. Choi, B. S. Parimalam, L. Su, B. Reeja-Jayan and S. Litster, *ACS Appl. Energy Mater.*, 2021, **4**, 1657–1665.
13 S. Haufe, R. Bernhard and J. Pfeiffer, *J. Electrochem. Soc.*, 2021, **168**, 080531.
14 F. Tariq, V. Yufit, D. S. Eastwood, Y. Merla, M. Biton, B. Wu, Z. Chen, K. Freedman, G. Offer, E. Peled, P. D. Lee, D. Golodnitsky and N. Brandon, *ECS Electrochem. Lett.*, 2014, **3**, A76.
15 J. P. Maranchi, A. F. Hepp, A. G. Evans, N. T. Nuhfer and P. N. Kumta, *J. Electrochem. Soc.*, 2006, **153**, A1246.
16 H. Jeon, I. Cho, H. Jo, K. Kim, M.-H. Ryou and Y. M. Lee, *RSC Adv.*, 2017, **7**, 35681–35686.
17 J. Schlaier, S. Cangaz, S. Maletti, C. Heubner, T. Abendroth, M. Schneider, S. Kaskel and A. Michaelis, *Adv. Mater. Interfaces*, 2022, **9**, 2200507.
18 S. Cangaz, O. Lohrberg, T. Abendroth, C. Heubner, F. Schmidt, H. Althues, S. Dörfler, A. Michaelis and S. Kaskel, *Adv. Mater. Interfaces*, 2023, **10**, 2202314.
19 X. Yu, Z. Feng, Y. Ren, D. Henn, Z. Wu, K. An, B. Wu, C. Fau, C. Li and S. J. Harris, *J. Electrochem. Soc.*, 2018, **165**, A1578.
20 D. Mishra, M. K. Jangid, S. Chhangani, P. Gandharapu, M. J. N. V. Prasad and A. Mukhopadhyay, *Energy Fuels*, 2020, **34**, 7763–7769.
21 M. E. Straumanis and L. S. Yu, *Acta Crystallogr.*, 1969, **25**, 676–682.
22 D. Anthony, D. Wong, D. Wetz and A. Jain, *Int. J. Heat Mass Transfer*, 2017, **111**, 223–231.
23 T. M. M. Heenan, I. Mombrini, A. Llewellyn, S. Checchia, C. Tan, M. J. Johnson, A. Jnawali, G. Garbarino, R. Jervis, D. J. L. Brett, M. Di Michiel and P. R. Shearing, *Nature*, 2023, **617**, 507–512.
24 H. D. Merchant, G. Khatibi and B. Weiss, *J. Mater. Sci.*, 2004, **39**, 4157–4170.
25 R. J. Tilley, *Understanding solids: the science of materials*, John Wiley & Sons, 2004.
26 A. Brennhagen, *DataverseNO*, 2025, DOI: **10.18710/MXJZMR**.
27 A. Brennhagen, D. Saha and A. Koposov, *ESRF*, 2027, DOI: **10.15151/ESRF-ES-1685306625**.
28 A. Brennhagen, I. C. Berdiell, A. Koposov and A. Pastusic, *ESRF*, 2028, DOI: **10.15151/ESRF-ES-2104236644**.